Cell Death & Differentiation (2021) 28:780–798
https://doi.org/10.1038/s41418-020-00623-9

Cell Death & Differentiation

ARTICLE

Thrombin-Par1 signaling axis disrupts COP9 signalosome subunit 3-mediated ABCA1 stabilization in inducing foam cell formation and atherogenesis

Monoranjan Boro[1] · Suresh Govatati[1] · Raj Kumar[1] · Nikhlesh K. Singh[1] · Prahalathan Pichavaram[1] · James G. Traylor Jr[2] · A. Wayne Orr[2] · Gadiparthi N. Rao[1]

Received: 18 December 2019 / Accepted: 7 September 2020 / Published online: 23 September 2020

Abstract

ATP-binding cassette transporters A1 (ABCA1) and G1 (ABCG1) play a vital role in promoting cholesterol efflux. Although, the dysregulation of these transporters was attributed as one of the mechanisms of atherogenesis, what renders their dysfunction is not well explored. Previously, we have reported that thrombin without having any effect on ABCG1 levels depletes ABCA1 levels affecting cholesterol efflux. In this study, we explored the mechanisms underlying thrombin-induced depletion of ABCA1 levels both in macrophages and smooth muscle cells. Under normal physiological conditions, COP9 signalosome subunit 3 (CSN3) was found to exist in complex with ABCA1 and in the presence of proatherogenic stimulants such as thrombin, ABCA1 was phosphorylated and dissociated from CSN3, leading to its degradation. Forced expression of CSN3 inhibited thrombin-induced ABCA1 ubiquitination and degradation, restored cholesterol efflux and suppressed foam cell formation. In Western diet (WD)-fed ApoE$^{-/-}$ mice, CSN3 was also disassociated from ABCA1 otherwise remained as a complex in Chow diet (CD)-fed ApoE$^{-/-}$ mice. Interestingly, depletion of CSN3 levels in WD-fed ApoE$^{-/-}$ mice significantly lowered ABCA1 levels, inhibited cholesterol efflux and intensified foam cell formation exacerbating the lipid laden atherosclerotic plaque formation. Mechanistic studies have revealed the involvement of Par1-Gα_{12}-Pyk2-Gab1-PKCθ signaling in triggering phosphorylation of ABCA1 and its disassociation from CSN3 curtailing cholesterol efflux and amplifying foam cell formation. In addition, although both CSN3 and ABCA1 were found to be colocalized in human non-lesion coronary arteries, their levels were decreased as well as dissociated from each other in advanced atherosclerotic lesions. Together, these observations reveal for the first time an anti-atherogenic role of CSN3 and hence, designing therapeutic drugs protecting its interactions with ABCA1 could be beneficial against atherosclerosis.

Introduction

Cholesterol is an essential component of cell membranes and a precursor for several hormones that are vital for body function [1]. However, excess cholesterol production can lead to its accumulation in peripheral tissues, including arteries where it becomes vulnerable for oxidation, esterification, and crystallization leading to foam cell formation and atherogenesis [2]. Therefore, removal of cholesterol from peripheral tissues is critical in the maintenance of cholesterol homeostasis [2]. ATP-binding cassette transporters A1 (ABCA1) and G1 (ABCG1) play an important role in the maintenance of cholesterol homeostasis by driving cholesterol efflux to apolipoprotein A-I (ApoA-I) and high-density lipoprotein (HDL), respectively, from peripheral tissues back to liver where it is converted to bile acids [3–5]. For example, mutation in ABCA1 gene causes

These authors contributed equally: Monoranjan Boro, Suresh Govatati

Edited by: D. Aberdam

Supplementary information The online version of this article (https://doi.org/10.1038/s41418-020-00623-9) contains supplementary material, which is available to authorized users.

✉ Gadiparthi N. Rao
rgadipar@uthsc.edu

[1] Department of Physiology, University of Tennessee Health Science Center, Memphis, TN 38163, USA

[2] Department of Pathology, Louisiana State University Health Science Center, Shreveport, LA 71103, USA

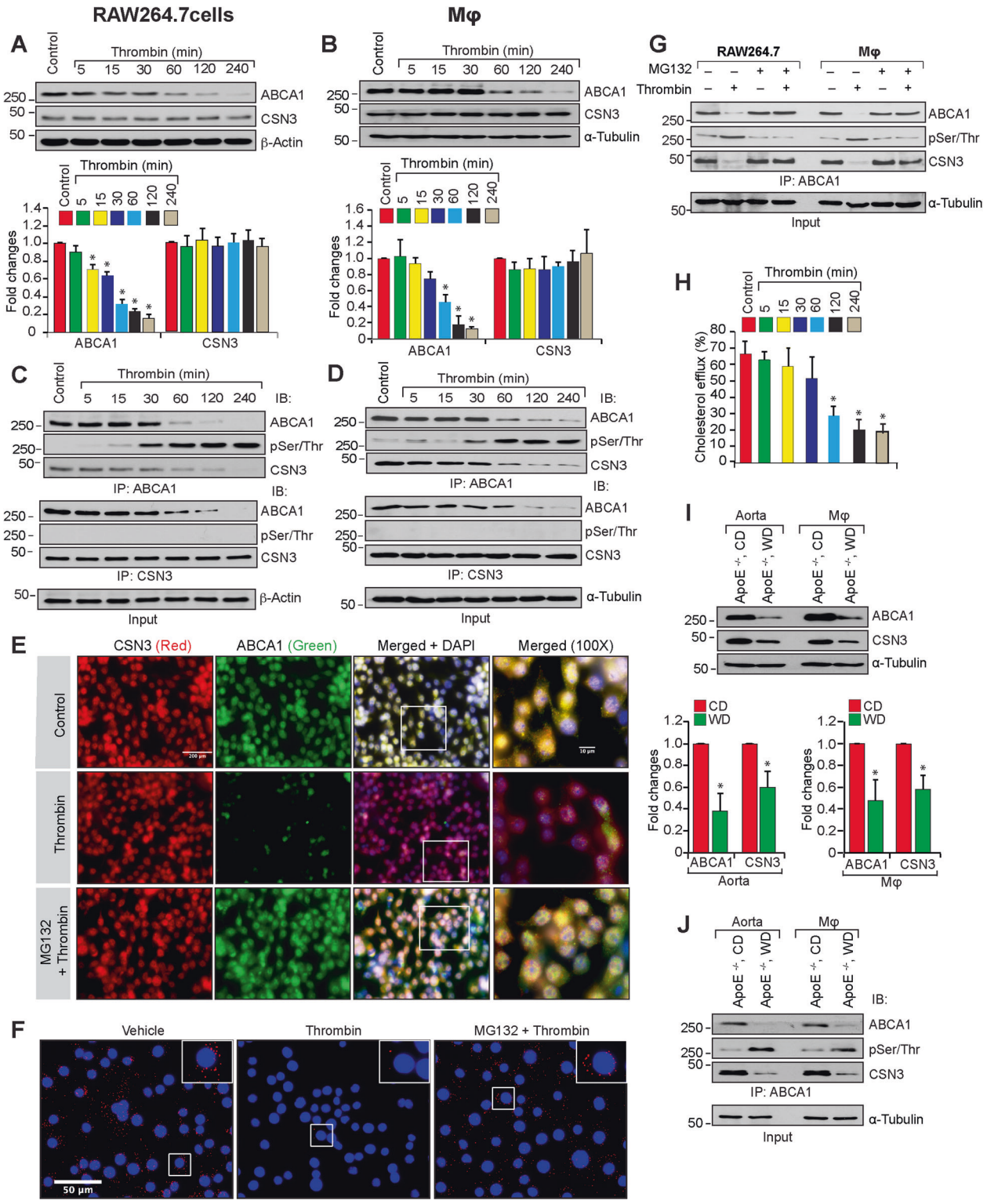

Tangier disease, which is characterized by low levels of HDL cholesterol (HDL-C) and ApoA-I and an increase in the accumulation of cholesteryl esters (CEs) within macrophage-rich tissues [6]. In addition, ABCA1 and ABCG1 were dysregulated during the pathogenesis of atherosclerosis [7–11]. Many reports have also shown that disruption of ABCA1 gene enhances atherosclerosis and inhibition of its proteasomal degradation restores cholesterol efflux and reduces atherosclerosis [12–14]. Recently, we reported that protease-activated receptor 1 (Par1)-

◀ **Fig. 1 Dissociation of CSN3 from ABCA1 in macrophages in response to thrombin and ApoE$^{-/-}$ mice in response to WD feeding. a–d** RAW264.7 cells **a**, **c** or peritoneal macrophages **b**, **d** were treated with and without thrombin (0.5 U/ml) for the indicated time periods, cell extracts were prepared and analyzed by western blotting for the indicated proteins using their specific antibodies **a**, **b** or immunoprecipitated with anti-ABCA1 or anti-CSN3 antibodies and the immunocomplexes were analyzed by western blotting for the indicated proteins using their specific antibodies **c**, **d**. Input protein from control and the indicated treatment in both **c**, **d** was immunoblotted for β-actin or α-tubulin. **e** Quiescent RAW264.7 cells were treated with and with without thrombin (0.5 U/ml) in the presence and absence of MG132 (10 μM) for 4 h, fixed and stained by double immunofluorescence for CSN3 and ABCA1. **f** Quiescent RAW264.7 cells were treated with and without thrombin (0.5 U/ml) in the presence and absence of MG132 (10 μM) for 4 h and subjected to in situ PLA as described in "Materials and Methods". **g** Quiescent RAW264.7 cells and peritoneal macrophages were treated with and without thrombin (0.5 U/ml) in the presence and absence of MG132 (10 μM) for 4 h, cell extracts prepared, immunoprecipitated with anti-ABCA1 antibodies and immunoblotted with the indicated antibodies. The input protein from these samples was immunoblotted for α-tubulin. **h** Peritoneal macrophages were treated with and without thrombin (0.5 U/ml) for the indicated time periods and cholesterol efflux to Apo-AI was measured. **i**, **j** ApoE$^{-/-}$ mice were fed with CD or WD for 10 weeks, aortas and macrophages were isolated, extracts were prepared and analyzed by western blotting for the indicated proteins using their specific antibodies **i** or immunoprecipitated with anti-ABCA1 antibodies and the immunocomplexes were analyzed by western blotting for the indicated proteins using their specific antibodies **j**. The input protein from each sample in **j** was immunoblotted for α-tubulin. The bar graph represents Mean ± SD values of three experiments. *$p < 0.01$ versus control or CD.

mediated atherogenesis was associated with ABCA1 proteasomal degradation, reduced cholesterol efflux and enhanced foam cell formation [15]. We have also shown that Par1-triggered ABCA1 depletion was dependent on Cullin3-mediated ubiquitination [15]. Based on these observations, we asked the question how ABCA1 is protected during normal physiological conditions? Previously, it was reported that COP9 signalosome subunit 2 (CSN2) and 5 (CSN5) upon forced expression were found to be co-precipitated with ABCA1 in HEK293 cells and CSN2 overexpression decreased ubiquitination of ABCA1 [16]. It was also reported that CSN5 expression increases in human atherosclerotic lesions and its deletion in ApoE$^{-/-}$ mice exacerbates atherogenesis in response to WD [17, 18]. Besides, it was demonstrated that COP9 signalosome subunit 3 (CSN3), another subunit of COP9 signalosome, binds with transcriptional factor interferon regulatory factor 5 and Ras guanine nucleotide exchange factor Sos1 and maintains their stability [19, 20]. In view of these observations and the fact that COP9 signalosome has a role in the deubiquitination and protection of proteins from proteasome-mediated degradation [21–23], we have studied the role of CSN3 in ABCA1 stability and cholesterol efflux. Here, we report for the first time that CSN3 interacts with and protects ABCA1 from thrombin and WD-induced degradation. Mechanistically, we found that thrombin via activation of Par1-Gα_{12}-Pyk2-Gab1-PKCθ signaling induces phosphorylation of ABCA1, leading to its disassociation from CSN3 and getting ubiquitinated and degraded. Furthermore, depletion of CSN3 levels in WD-fed ApoE$^{-/-}$ mice substantially decreased ABCA1 levels as compared with those that received control siRNA, leading to heightened foam cell formation and atherosclerotic lesion progression in response to WD. Based on these findings, we believe that CSN3 plays an atheroprotective role and hence, developing therapeutic drugs to safeguard CSN3–ABCA1 complex would be useful in controlling atherogenesis.

Results

Disruption of CSN3 and ABCA1 interactions in macrophages in response to thrombin and in ApoE−/− mice in response to WD

Previously, we reported that Cullin3 mediates ABCA1 ubiquitination and its proteasomal degradation [15]. COP9 signalosome by deneddylation of Cullins has a role in protein stability [21–23]. As CSN3 maintains the stability of several proteins [19, 20], here we tested its role in ABCA1 stability. Thrombin, a G protein-coupled receptor agonist, while depleting ABCA1 levels had no effect on steady state CSN3 levels (Fig. 1a, b). Next, we found that both CSN3 and ABCA1 exist as a complex in control cells and in response to thrombin CSN3 was found to be dissociated from ABCA1 (Fig. 1c, d). To understand the mechanisms underlying CSN3 dissociation from ABCA1, we tested the effect of thrombin on ABCA1 phosphorylation. Thrombin-induced ABCA1 phosphorylation in a manner that precedes its dissociation from CSN3 (Fig. 1c, d). Furthermore, consistent with co-immunoprecipitation (co-IP) findings, co-immunofluorescence staining confirmed that CSN3 and ABCA1 exist as a complex in control cells, and in response to thrombin they were found to be dissociated from each other and ABCA1 levels were decreased (Fig. 1e). In addition, in the presence of proteasomal inhibitor, MG132 [24], thrombin failed to deplete ABCA1 levels and both CSN3 and ABCA1 were found to be colocalized (Fig. 1e). The interactions between CSN3 and ABCA1 were further confirmed by in situ proximity ligation assay (PLA). Basically, PLA results showed that CSN3 and ABCA1 exist as a complex in control cells, which was completely disrupted in response to thrombin (Fig. 1f). Besides, in line with the co-immunofluorescence findings, in the presence of MG132, thrombin did not lead to the dissociation of CSN3 from ABCA1 (Fig. 1f). We also studied the effect of thrombin on CSN3 and ABCA1 interactions in the presence and absence of MG132 by co-IP

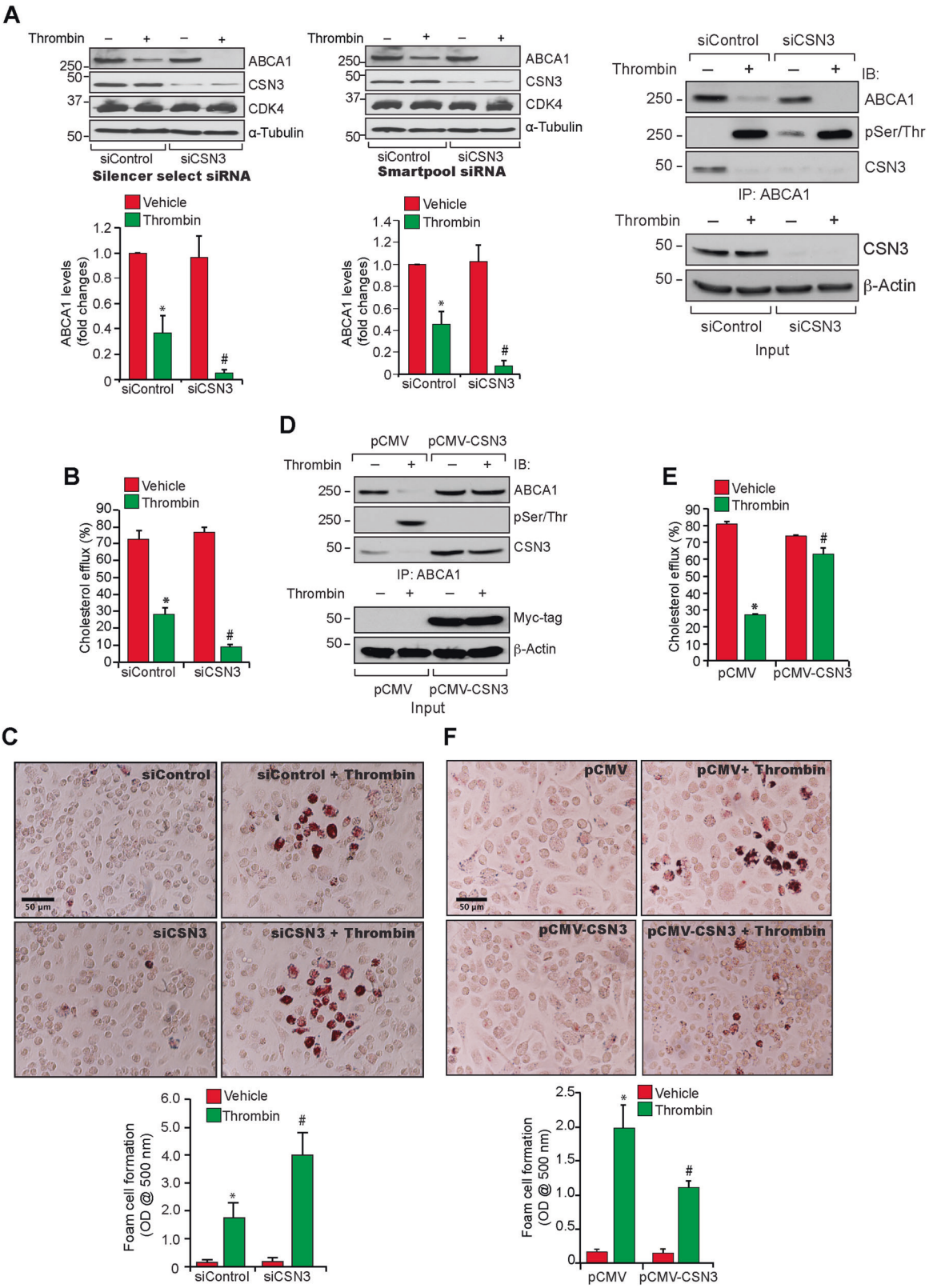

experiments. First, thrombin-induced degradation of ABCA1 was completely prevented by MG132 (Fig. 1g). Second, inhibition of ABCA1 degradation by MG132 restored its interaction with CSN3 (Fig. 1g). Third, the rescue of ABCA1 interaction with CSN3 was also correlated with the suppression of ABCA1 phosphorylation

◀ **Fig. 2 CSN3 blocks thrombin-induced ABCA1 depletion, rescues cholesterol efflux, and inhibits foam cell formation. a** (left and middle panels) RAW264.7 cells were transfected with the indicated siControl or siCSN3 (100 nmoles), treated with and without thrombin (0.5 U/ml) for 4 h, cell extracts were prepared and analyzed by western blotting for the indicated proteins using their specific antibodies. **a** (right panel) RAW264.7 cells that were transfected with siControl or siCSN3 (100 nmoles) were treated with and without thrombin for 4 h, cell extracts prepared, immunoprecipitated with anti-ABCA1 antibodies and the immunocomplexes were immunoblotted sequentially with pSer/Thr, CSN3, and ABCA1 antibodies. **b**, **c** RAW264.7 cells were transfected with silencer select siControl or siCSN3, treated with and without thrombin (0.5 U/ml) for 4 h and assayed for cholesterol efflux **b** or foam cell formation **c**. **d** RAW264.7 cells were transfected with pCMV or pCMV-CSN3 plasmid, treated with and without thrombin (0.5 U/ml) for 4 h, cell extracts were prepared, immunoprecipitated with anti-ABCA1 antibodies and immunoblotted with the indicated antibodies. The input protein from each sample was immunoblotted for CSN3 or α-tubulin. **e**, **f** All the conditions were the same as in **d** except that cells were assayed for cholesterol efflux **e** or foam cell formation **f**. The bar graphs represent Mean ± SD values of three experiments. $^{*}p < 0.01$ versus siControl + vehicle or pCMV + vehicle, $^{\#}p < 0.01$ versus siControl + thrombin or pCMV + thrombin.

(Fig. 1g). Thus, the observations by co-IP, co-immunofluorescence and PLA along with MG132 rescue experiments clearly demonstrate that CSN3 and ABCA1 exist as a complex under basal conditions and that their interactions disrupt in response to thrombin. Consistent with its effect on ABCA1 depletion, thrombin also decreased cholesterol efflux (Fig. 1h). Based on these results, we conclude that CSN3 exists in complex with ABCA1 and maintains its stability under normal conditions in macrophages, which is disrupted in response to thrombin. To validate these results in vivo, ApoE$^{-/-}$ mice were fed with WD for 10 weeks or left on CD and ABCA1 and CSN3 levels were measured both in aorta and macrophages. Both ABCA1 and CSN3 levels were found to be decreased in aorta as well as macrophages of WD-fed ApoE$^{-/-}$ mice as compared with those of CD-fed ApoE$^{-/-}$ mice (Fig. 1i). In addition, ABCA1 was found to be phosphorylated and dissociated from CSN3 both in aorta and macrophages of WD-fed ApoE$^{-/-}$ mice as compared with those of CD-fed ApoE$^{-/-}$ mice (Fig. 1j). These results demonstrate that WD triggers phosphorylation of ABCA1 and its dissociation from CSN3, leading to its degradation in ApoE$^{-/-}$ mice.

CSN3 rescues cholesterol efflux from inhibition by thrombin and reduces foam cell formation

To gain further evidence for the possible role of CSN3 in ABCA1 stability, we used siRNA approach. Downregulation of CSN3 levels by its siRNA in RAW264.7 cells enhanced thrombin-induced degradation of ABCA1 as well as exacerbated thrombin-induced inhibition of cholesterol efflux (Fig. 2a, left and middle panels and b). Furthermore, CSN3 depletion also correlated with a slight increase in thrombin-induced ABCA1 phosphorylation (Fig. 2a, right panel). As the effects of thrombin on ABCA1 depletion were dependent on CSN3 dissociation from ABCA1, downregulation of CSN3 levels as expected resulted no substantial additive effects on ABCA1 phosphorylation and degradation. However, downregulation of CSN3 levels alone caused an increase in ABCA1 phosphorylation and its degradation (Fig. 2a, right panel). In line with these observations, CSN3 depletion enhanced thrombin-induced foam cell formation (Fig. 2c). On the other hand, overexpression of CSN3 in RAW264.7 cells restored CSN3 association with ABCA1 from thrombin-induced dissociation and prevented thrombin-induced phosphorylation and degradation of ABCA1 (Fig. 2d). Overexpression of CSN3 also restored cholesterol efflux from inhibition by thrombin and prevented thrombin-induced foam cell formation (Fig. 2e, f). Together, these findings demonstrate that CSN3 maintains ABCA1 stability, promotes cholesterol efflux and decreases foam cell formation.

Depletion of CSN3 in ApoE$^{-/-}$ mice reduces ABCA1 levels, inhibits cholesterol efflux, and increases foam cell formation

Based on our in vitro results showing the protective role of CSN3 on ABCA1 stability, we tested whether depletion of CSN3 levels leads to ABCA1 downregulation in WD-fed ApoE$^{-/-}$ mice. Considering that homozygous deletion of CSN3 is embryonic lethal [25], we applied in vivo siRNA approach. To this end, siControl (control siRNA) or siCSN3 was injected intravenously into ApoE$^{-/-}$ mice and at the indicated time periods of post injection, CSN3 levels were measured in aorta. CSN3 levels were significantly reduced in aorta of ApoE$^{-/-}$ mice at 7 days post injection of its siRNA (Fig. 3a). Based on this observation, ApoE$^{-/-}$ mice were fed with WD for 10 weeks and siControl or siCSN3 was given every 7 days for the duration of the feeding. As expected, CSN3 levels were substantially depleted in aorta and macrophages of WD-fed ApoE$^{-/-}$ mice injected with siCSN3 as compared with those mice that received siControl (Fig. 3b, c). In addition, ABCA1 but not ABCG1 or CD36 levels were found to be substantially reduced in siCSN3 received WD-fed ApoE$^{-/-}$ mice as compared with ApoE$^{-/-}$ mice that received siControl (Fig. 3b–e). Furthermore, depletion of CSN3 levels inhibited cholesterol efflux to ApoA-I in peritoneal macrophages of WD-fed ApoE$^{-/-}$ mice and as a consequence increased the capacity of their foam cell formation as compared with those of siControl received mice (Fig. 3f, g). Together, these results demonstrate that depletion of CSN3 levels in WD-fed ApoE$^{-/-}$ mice reduces ABCA1 levels, inhibits cholesterol efflux, and increases foam cell formation.

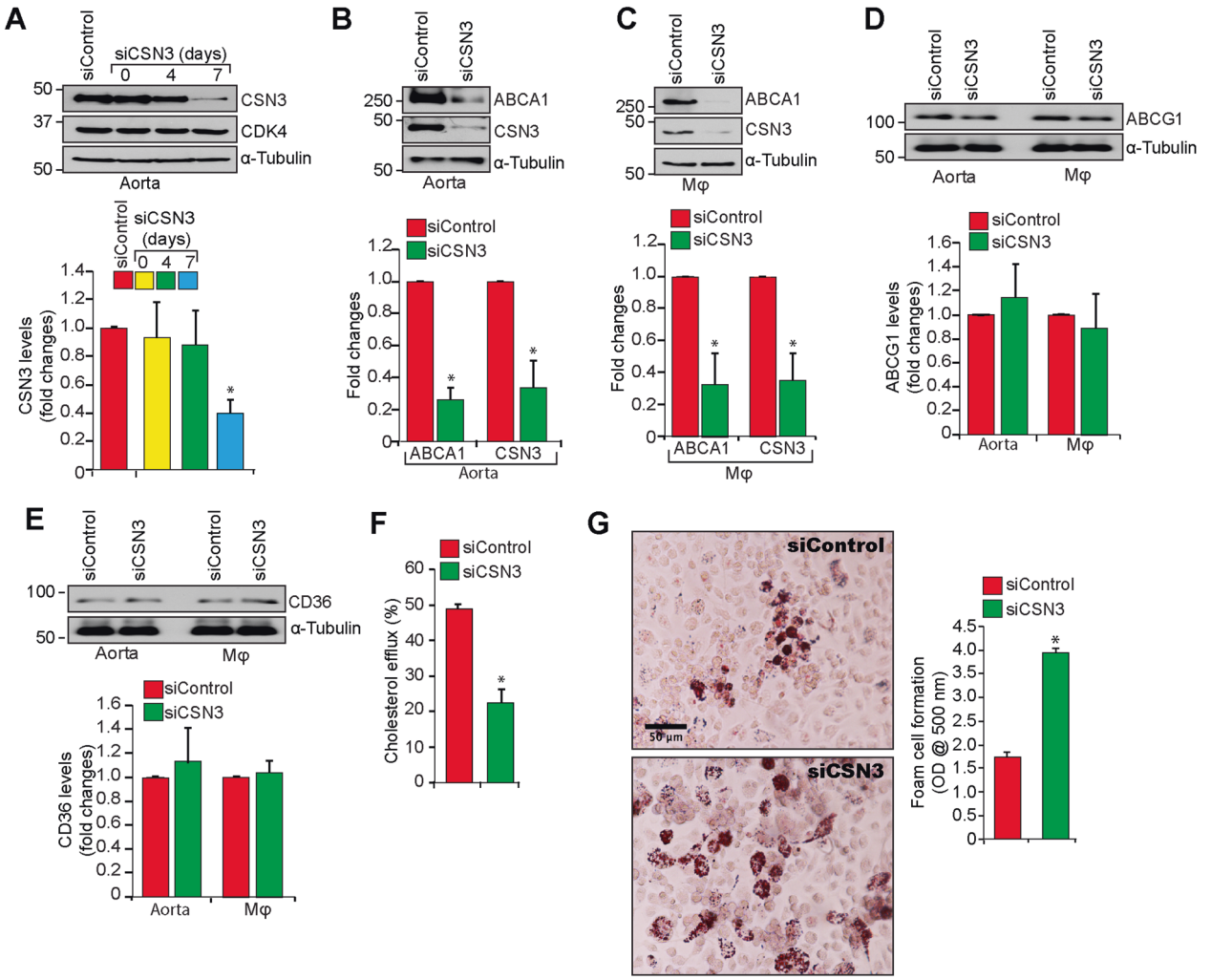

Fig. 3 Downregulation of CSN3 depletes ABCA1 levels, inhibits cholesterol efflux, and enhances foam cell formation in WD-fed ApoE$^{-/-}$ mice. a ApoE$^{-/-}$ mice were injected (iv) with siControl or siCSN3 (40 μg/mice), killed at the indicated days, aortas were dissected out, tissue extracts were prepared and analyzed by western blotting for CSN3 levels using its specific antibody. The blot was reprobed sequentially for CDK4 and α-tubulin to show the effect of the siRNA on its off-target molecules. **b–e** ApoE$^{-/-}$ mice were fed with CD or WD for 10 weeks and injected (iv) with siControl or siCSN3 every 7 days for the entire duration of the feeding, following which aortas and peritoneal macrophages were isolated, extracts were prepared and analyzed by western blotting for the indicated proteins using their specific antibodies. **f**, **g**. All the conditions were the same as in **c** except that macrophages were assayed for cholesterol efflux **f** and foam cell formation **g**. The bar graphs represent mean ± SD values of three experiments. *$p < 0.01$ versus siControl.

Table 1 Plasma lipid profile of ApoE$^{-/-}$ mice that were fed with WD for 10 weeks and given the i.v. injections of the indicated siRNA.

Genotype	Diet	Weight (gm)	Cholesterol mg/dl	LDL mg/dl	Triglycerides mg/dl	n
ApoE$^{-/-}$ + siControl	WD	36 ± 1	222 ± 49	114 ± 54	126 ± 32	8
ApoE$^{-/-}$ + siCSN3	WD	37 ± 2	355 ± 54*	195 ± 60*	133 ± 48	8

*$p < 0.01$ versus siControl.

Depletion of CSN3 levels in WD-fed ApoE$^{-/-}$ mice accelerates atherosclerotic lesions

To test the role of CSN3 in atherosclerosis, ApoE$^{-/-}$ mice were fed with WD for 10 weeks and given control or CSN3 siRNA every 7 days for the duration of the feeding and lesion development was analyzed by Oil Red O staining of aorta and aortic root cross-sections. Although no significant differences were found in the body weight and TG levels between siControl and siCSN3 injected WD-fed ApoE$^{-/-}$ mice, total cholesterol and LDL levels were found to be substantially increased in the latter group as compared with the former group of mice (Table 1). Measurement of total atherosclerotic lesion area by enface staining revealed a significant increase in the lesions in the aorta of siCSN3 received ApoE$^{-/-}$ mice (Fig. 4a). The percentage of plaque

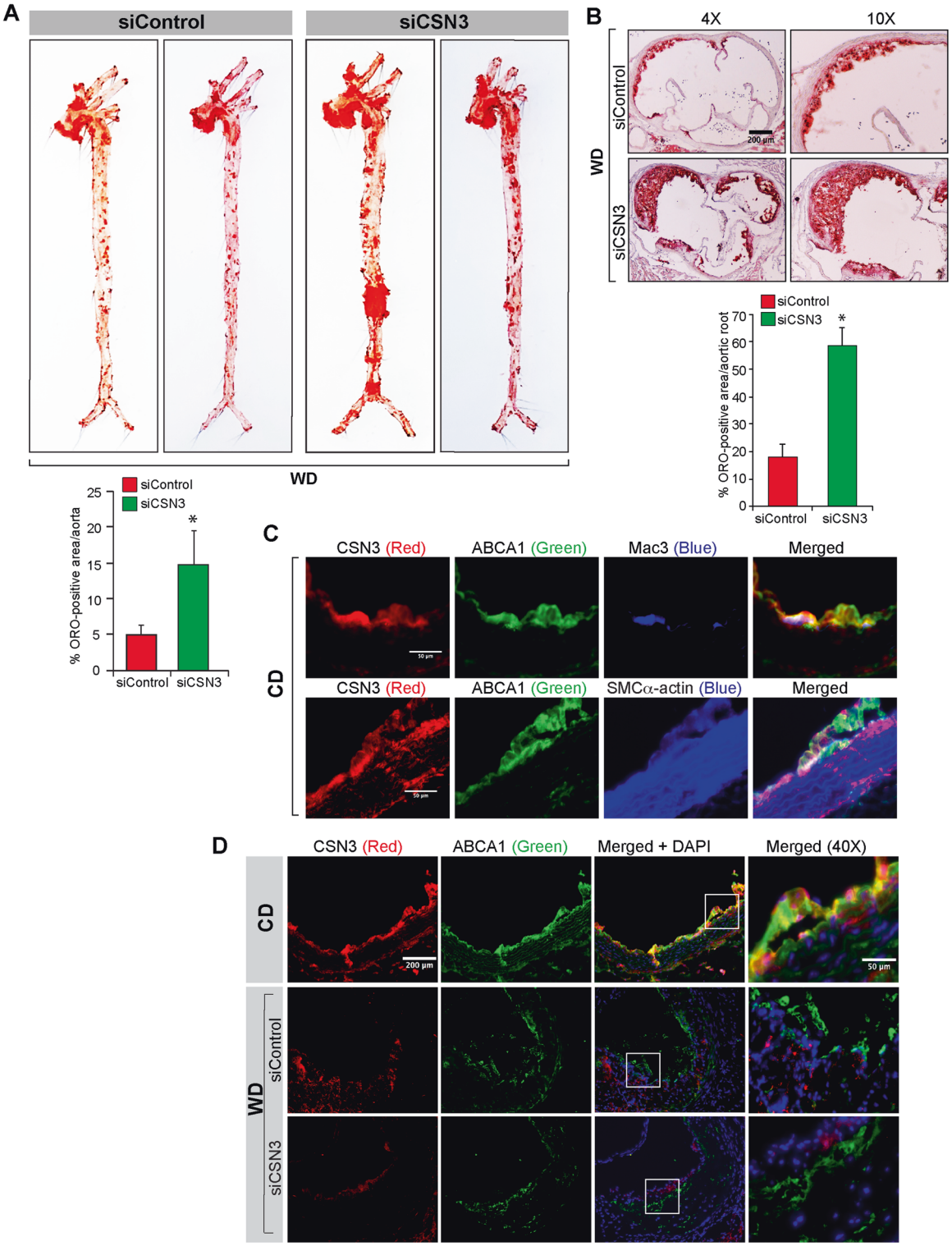

area in the aortic roots of WD-fed ApoE$^{-/-}$ mice that received siCSN3 was also increased significantly as compared with ApoE$^{-/-}$ mice that received siControl (Fig. 4b). Immunofluorescence staining of the aortic root cross-sections while showing colocalization of CSN3 with ABCA1 in both macrophages and VSMCs of CD-fed ApoE$^{-/-}$ mice (Fig. 4c), these molecules were found to be dissociated from each other in WD-fed ApoE$^{-/-}$ mice (Fig. 4d). Furthermore, both CSN3 and ABCA1 levels were found to be substantially decreased in the aortic root

◀ **Fig. 4 Depletion of CSN3 levels exacerbates WD-induced atherosclerotic lesions in ApoE$^{-/-}$ mice. a** Representative enface staining of aortas from 10 weeks of WD-fed ApoE$^{-/-}$ mice that received either siControl or siCSN3. The bar graph shows % Oil Red O (ORO)-positive area/aorta. **b** Representative Oil red O staining of the aortic root cross-sections of the mice described in **a** are shown and the bar graph shows the % ORO-positive area/aortic root. **c** Aortic root cross-sections of CD-fed ApoE$^{-/-}$ mice were coimmunostained for SMCα-actin or Mac3 in combination with CSN3 and ABCA1. **d** The aortic root cross-sections of ApoE$^{-/-}$ mice that were fed with either WD and received intravenously either siControl or siCSN3 or left on CD for 10 weeks were analyzed by double immunofluorescence staining for CSN3 and ABCA1. The bar graphs represent Mean ± S.D. values of seven animals. *$p < 0.01$ versus siControl. Scale bars in **b** are 200 μm, **c** are 50 μm and **d** far left and far right are 200 μm and 50 μm, respectively.

cross-sections of WD-fed ApoE$^{-/-}$ mice as compared with CD-fed ApoE$^{-/-}$ mice and this depletion was even more prominent in WD-fed ApoE$^{-/-}$ mice in which CSN3 levels were depleted by its siRNA (Fig. 4d).

Role of Par1-Gα$_{12}$-Pyk2-Gab1-PKCθ signaling axis in thrombin-induced disruption of ABCA1 and CSN3 complex, inhibition of cholesterol efflux and increase in foam cell formation

Having found the atheroprotective role of CSN3 in vitro and in vivo, we next explored the mechanism underlying thrombin-induced disassociation of CSN3 from ABCA1. Previously, we have shown that thrombin engages Par1-mediated Gα$_{12}$-Pyk2-Gab1-PKCθ signaling axis in the ubiquitination and degradation of ABCA1 by Cullin3 in promoting atherogenesis [15]. Therefore, we have examined whether thrombin-induced dissociation of CSN3 from ABCA1 was also dependent on Par1-Gα$_{12}$-Pyk2-Gab1-PKCθ signaling axis. Indeed, the genetic loss of Par1 or PKCθ gene or siRNA-mediated depletion of Gα$_{12}$, Pyk2 or Gab1 levels suppressed thrombin-induced phosphorylation of ABCA1 and its dissociation from CSN3, restoring its stabilization (Fig. 5a). Consistent with these observations, genetic disruption of Par1 or PKCθ gene or siRNA-mediated downregulation of Gα$_{12}$, Pyk2 or Gab1 also restored cholesterol efflux from inhibition by thrombin and attenuated foam cell formation (Fig. 5b, c).

Thrombin disrupts CSN3 interaction with ABCA1, leading to its degradation and a reduction in cholesterol efflux in smooth muscle cells

Many studies have shown that besides macrophages, vascular smooth muscle cells (VSMCs) also play a role in foam cell formation and atherogenesis [26, 27]. In order to find whether thrombin induces ABCA1 depletion, if it does, whether it was due to disruption of ABCA1/CSN3 complex in VSMCs, first we studied a time-course effect of thrombin on ABCA1 levels. Thrombin-induced depletion of ABCA1 levels in a time-dependent manner in mouse VSMCs and it was correlated with its phosphorylation and dissociation from CSN3 (Fig. 6a). Consistent with these observations, thrombin also inhibited cholesterol efflux in VSMCs in a time-dependent manner (Fig. 6b). In addition, down-regulation of CSN3 levels using its siRNA enhanced thrombin-induced ABCA1 depletion and accordingly inhibited cholesterol efflux (Fig. 6c, d). On the other hand, overexpression of CSN3 protected ABCA1 from thrombin-induced depletion and restored cholesterol efflux (Fig. 6e, f). Furthermore, although siRNA-mediated depletion of CSN3 levels enhanced thrombin-induced foam cell formation, CSN3 overexpression substantially reduced this effect (Fig. 6g, h). To find whether Par1-Gα$_{12}$-Pyk2-Gab1-PKCθ signaling has a role in thrombin-induced phosphorylation of ABCA1 and its dissociation from CSN3 in VSMCs, we have depleted the levels of these molecules in VSMCs using their respective siRNAs, treated cells with and without thrombin (0.5 U/ml) for 4 h, cell extracts were prepared and analyzed for ABCA1 phosphorylation and its dissociation from CSN3. Thrombin-induced ABCA1 phosphorylation and its dissociation from CSN3 and depletion of Par1, Gα$_{12}$, Pyk2, Gab1, or PKCθ levels abrogated these effects (Fig. 7a, b). Consistent with these observations, depletion of Par1, Gα$_{12}$, Pyk2, Gab1, or PKCθ levels in VSMCs also rescued cholesterol efflux from inhibition by thrombin (Fig. 7c). Similarly, depletion of Par1, Gα$_{12}$, Pyk2, Gab1, or PKCθ levels prevented thrombin-induced foam cell formation of VSMCs (Fig. 7d). In addition, proteasomal inhibitor, MG132, prevented thrombin-induced depletion of ABCA1 and this effect was associated with decreased ABCA1 phosphorylation and its increased association with CSN3 (Fig. 7e). Previously, we have demonstrated that Cullin3 ubiquitinates and degrades ABCA1 in response to thrombin [15]. Based on these observations, we asked the question whether overexpression of CSN3 prevents thrombin-induced association of Cullin3 with ABCA1, leading to diminished ABCA1 ubiquitination and degradation. First, forced expression of CSN3 prevented thrombin-induced association of Cullin3 with ABCA1 in macrophages (Fig. 7f). Second, forced expression of CSN3 also blocked thrombin-induced phosphorylation of ABCA1 (Fig. 7f). Third, in line with these observations, forced expression of CSN3 diminished ABCA1 ubiquitination and its degradation both in macrophages and VSMCs (Fig. 7g). Besides these observations, in the presence of MG132, whereas thrombin-induced ABCA1 phosphorylation and ubiquitination were substantially reduced, CSN3 was found to be associated with ABCA1 (Fig. 7h). In addition, thrombin-induced ABCA1 phosphorylation and ubiquitination were also correlated by its association with Cullin3

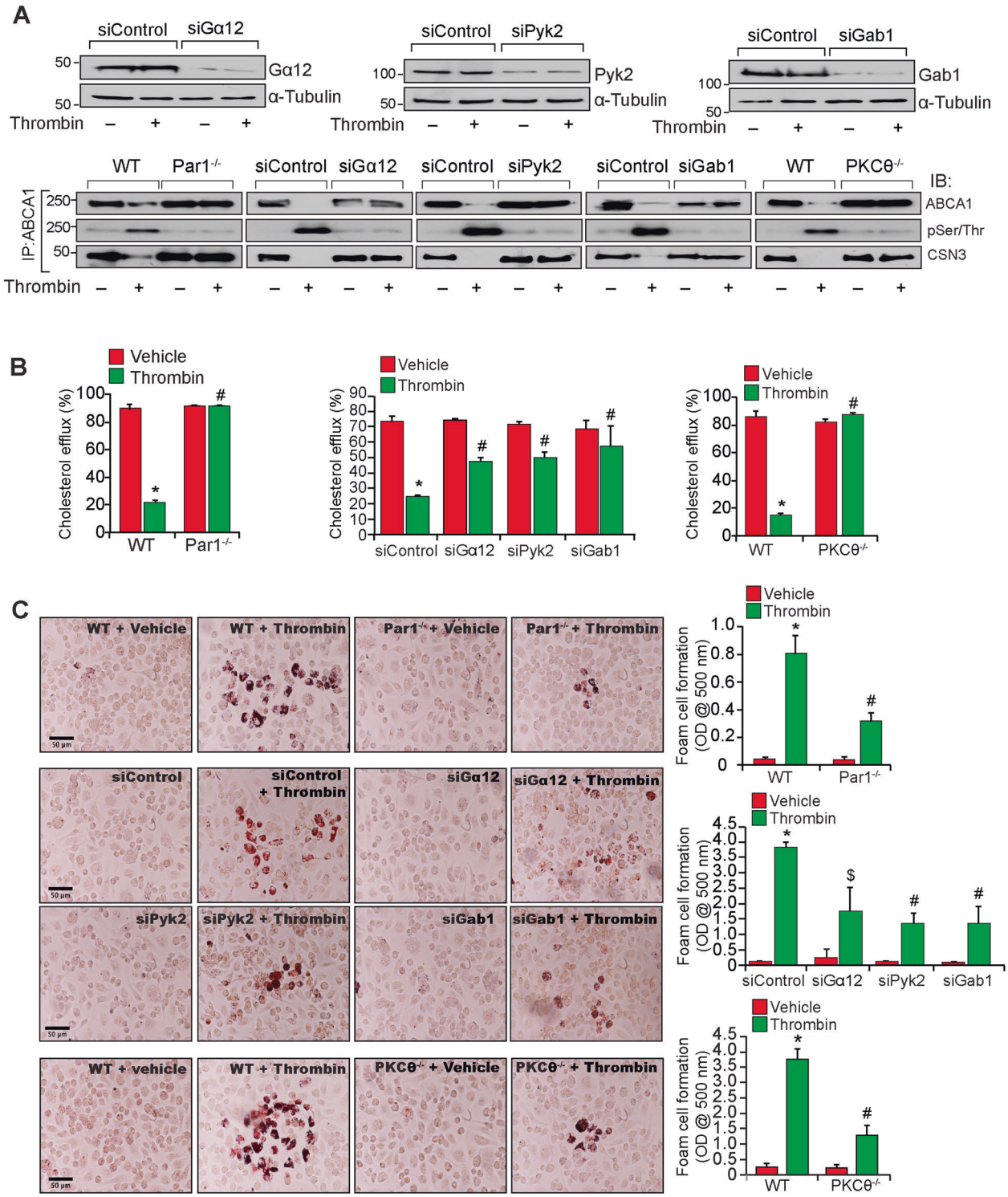

Fig. 5 Role of Par1-Gα12-Pyk2-Gab1-PKCθ signaling in thrombin-induced disassociation of ABCA1 and CSN3 complex and inhibition of cholesterol efflux and foam cell formation. **a** RAW264.7 cells that were transfected with the indicated siRNAs or Par1$^{-/-}$ or PKCθ$^{-/-}$ mouse peritoneal macrophages were quiesced, treated with and without thrombin (0.5 U/ml) for 4 h, cell extracts prepared, immunoprecipitated with anti-ABCA1 antibody and the immunocomplexes were analyzed by western blotting for the indicated proteins (bottom row panels). Top row panels show the efficacy of the siRNAs on their target and off-target molecules. **b**, **c** All the conditions were the same as in bottom row **a** except that cells were assayed for cholesterol efflux **b** or foam cell formation **c**. The bar graphs represent mean ± SD values of three experiments. *$p < 0.01$ versus vehicle, or siControl + vehicle; $^{\#}p < 0.01$ versus WT + Thrombin or siControl + Thrombin; $^{\$}p < 0.05$ versus siControl + Thrombin.

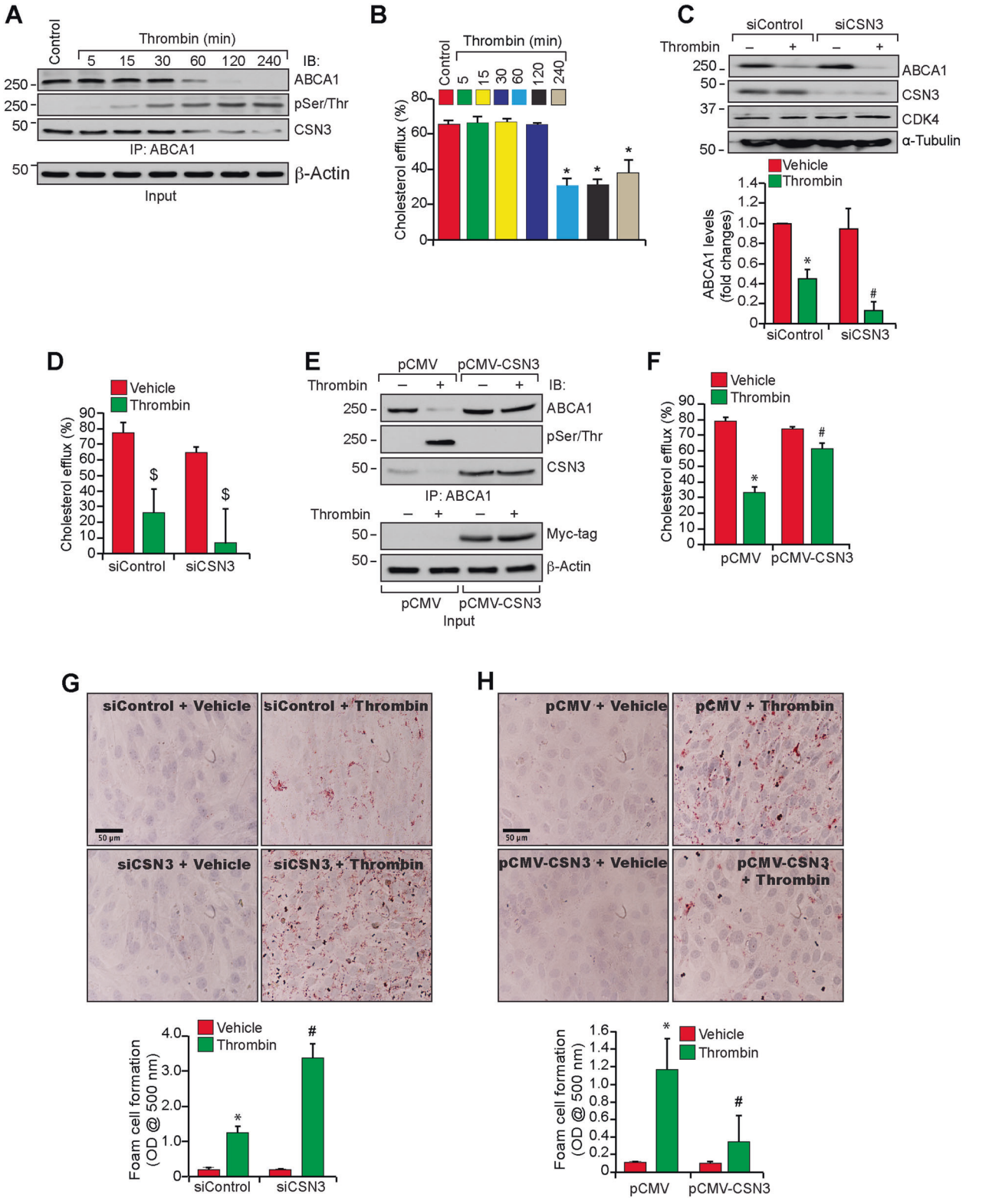

(Fig. 7h). To find whether CSN3 protects ABCA1 as part of CSN holo-complex, we examined for the interaction of other members of CSN complex, such as CSN1, CSN2, and CSN4 with ABCA1. First, thrombin time-course experiment revealed that, consistent with CSN3 levels, thrombin had no effect on the steady state levels of CSN1, CSN2, or CSN4 levels (Supplementary Figure 1a). Second, besides CSN3, CSN1, CSN2, and CSN4 were found to exist

◀ **Fig. 6 Thrombin induces dissociation of CSN3 from ABCA1, leading to ABCA1 depletion and inhibition of cholesterol efflux in MASMCs. a** Quiescent MASMCs were treated with and without thrombin (0.5 U/ml) for the indicated time periods, cell extracts prepared, immunoprecipitated with anti-ABCA1 antibodies and the immunocomplexes were analyzed by western blotting using anti-ABCA1, anti-pSer/Thr, or anti-CSN3 antibodies. The input protein from each sample was immunoprobed for β-actin. **b** Quiescent MASMCs were treated with and without thrombin (0.5 U/ml) for the indicated time periods and assayed for cholesterol efflux. **c–h** MASMCs that were transfected with siControl or siCSN3 or pCMV or pCMV-CSN3 were treated with and without thrombin (0.5 U/ml) for 4 h and either cell extracts were prepared and analyzed by western blotting for the indicated proteins using their specific antibodies **c** or immunoprecipitated with anti-ABCA1 antibodies and the immunocomplexes were analyzed by western blotting using anti-ABCA1, anti-pSer/Thr or anti-CSN3 antibodies **e** or assayed for cholesterol efflux **d**, **f** or foam cell formation **g**, **h**. $^{*}p < 0.01$ versus control, siControl + vehicle or pCMV + vehicle, $^{\#}p < 0.01$ versus

in complex with ABCA1 in control cells and in response to thrombin ABCA1 was found to be phosphorylated, dissociated from CSN1, CSN2, and CSN4 and decreased in its steady state levels and all these effects were prevented in the presence of proteasomal inhibitor, MG132 (Supplementary Figure 1b).

Depletion of CSN3 and ABCA1 levels in advanced atherosclerotic lesions of human coronary artery

To extrapolate the observations of mouse atherosclerotic model to human atherosclerosis, we examined the interactions between CSN3 and ABCA1 in human non-lesion and lesion containing coronary artery sections by coimmunostaining. It is interesting to note that in arteries with no lesions or minimal lesions (grade II) both CSN3 and ABCA1 were found to be colocalized (Fig. 8). On the other hand, both these molecules were found to be decreased as well as dissociated from each other in human coronary arteries with advanced lesions (Fig. 8).

Discussion

ABCA1 has a crucial role in reducing the risk of atherogenesis by mediating cholesterol efflux [4, 5, 28–32]. Although, the role of ABCA1 in promoting cholesterol efflux is well appreciated [4, 28], the biochemical mechanisms regulating the steady state ABCA1 levels and its functions during normal and pathological conditions were not completely understood. In this study, we attempted to understand the molecular mechanisms underlying the regulation of ABCA1 levels during normal and atherogenic conditions. Our results demonstrate that CSN3, which exists in complex with ABCA1 in normal condition becomes dissociated from the transporter, thereby triggering its ubiquitination and degradation, inhibiting cholesterol efflux and promoting foam cell formation both in vitro in macrophages in response to thrombin and in vivo in ApoE$^{-/-}$ mice in response to WD. Interestingly, CSN5, another component of COP9 signalosome, was also reported to protect against atherosclerosis via inhibition of NFκB [18]. In addition, upon forced expression, both CSN2 and CSN5 were shown to modulate deubiquitination of ABCA1 in HEK293 cells [16]. Previously, we have shown that thrombin induces Cullin3-mediated ubiquitination and degradation of ABCA1, leading to inhibition of cholesterol efflux [15]. Based on our results as well as others, we believe that CSN3 could protect ABCA1 from ubiquitination and degradation as the role of CSN in promoting deubiquitination was well established [16, 22, 33].

Although a previous study showed that CSN2 and CSN5 when overexpressed in HEK293 cells can form a complex with ABCA1 [16], their role in atherogenesis is mostly unknown till recently when deletion of CSN5 was reported to exacerbate atherogenesis [18]. Hence, we assessed the role of CSN3 in regulating atherogenesis by examining its impact on cholesterol efflux and foam cell formation in response to atherogenic stimulants such as thrombin in vitro and WD feeding in vivo. In this context, overexpression of CSN3 in macrophages inhibited thrombin-induced ABCA1 degradation, increased cholesterol efflux and decreased foam cell formation while downregulation of its levels further enhanced thrombin-induced ABCA1 degradation, inhibited cholesterol efflux, and heightened foam cell formation than without CSN3 depletion. Furthermore, depletion of CSN3 levels in WD-fed ApoE$^{-/-}$ mice reduced ABCA1 levels, curtailed cholesterol efflux, and increased foam cell formation with enhanced atherosclerotic lesion formation. Interestingly, serum cholesterol levels were found to be increased in WD-fed ApoE$^{-/-}$ mice in which CSN3 levels were depleted by its siRNA as compared with those received control non-targeting siRNA. However, downregulation of ABCA1 levels would be expected to lower serum cholesterol levels owing to decreased cholesterol efflux. Indeed, it was reported that disruption of ABCA1 gene in ApoE$^{-/-}$ mice leads to decreased serum cholesterol levels in response to WD [34]. On the other hand, another study has shown that treatment of cholesterol-rich diet-fed ApoE$^{-/-}$ mice with hydrogen sulfide donor NaHS increases ABCA1 levels, leading to decreased serum cholesterol and LDL levels and reduced lesion severity [35]. Based on these observations as well as our findings, it may be suggested that depletion of CSN3 levels, besides downregulating ABCA1 levels, may also influence cholesterol synthesis or its intestinal absorption, leading to its increased serum levels, which in turn, may trigger to elevate LDL levels. Mechanistic studies have revealed that CSN3

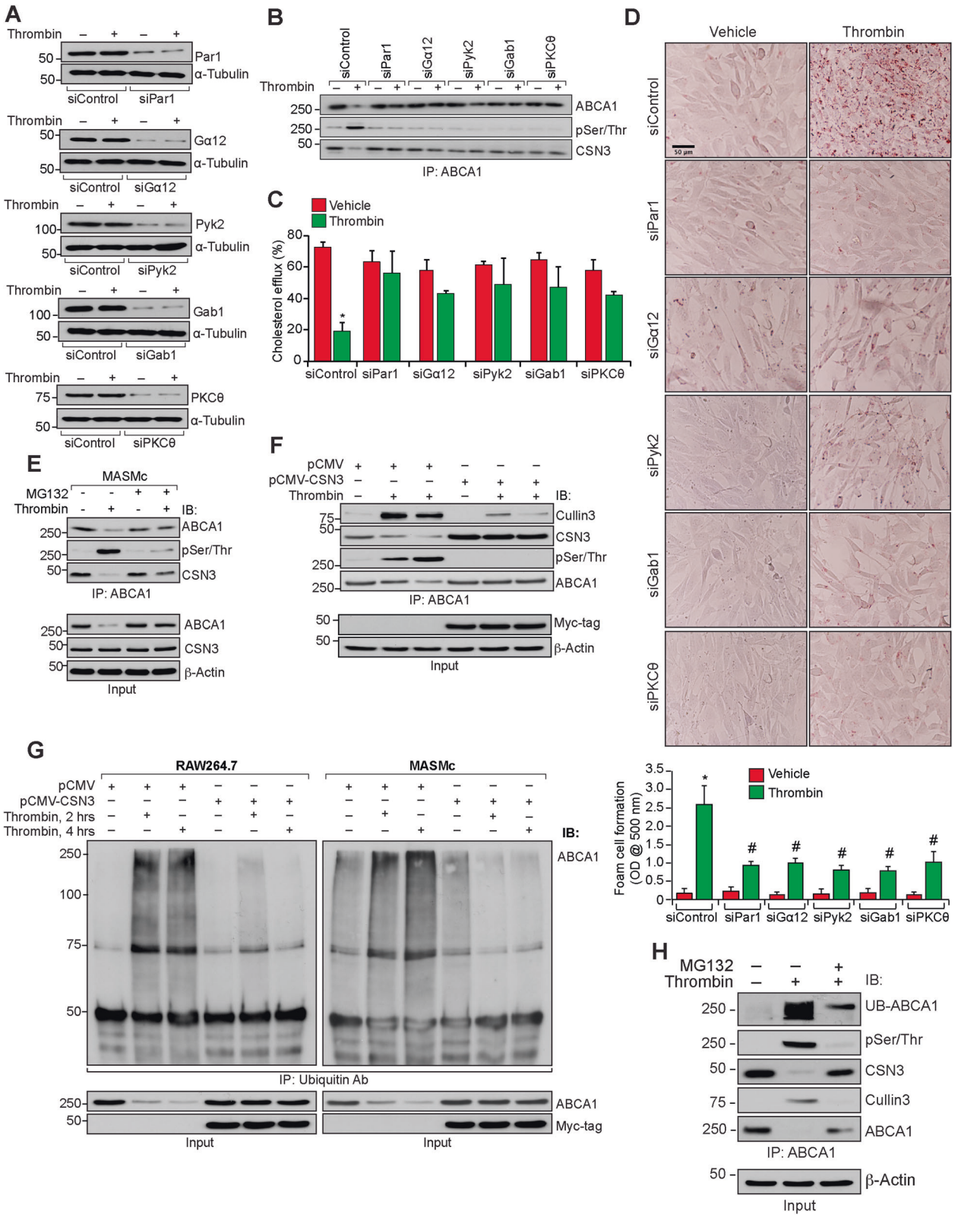

dissociation from ABCA1, decreased cholesterol efflux, and increased foam cell formation by thrombin were dependent on activation of Par1-Gα_{12}-Pyk2-Gab1-PKCθ signaling axis. Previously, we have reported that PKCθ phosphorylates ABCA1 on Ser/Thr residues and its phosphorylation appears to be involved in its ubiquitination by Cullin3 and

◀ **Fig. 7 Role of Par1-Gα12-Pyk2-Gab1-PKCθ signaling in thrombin-induced disassociation of CSN3 from ABCA1 and inhibition of cholesterol efflux and foam cell formation in MASMCs. a**, **b** MASMCs were transfected with the indicated siRNA, quiesced, treated with and without thrombin (0.5 U/ml) for 4 h, cell extracts prepared and either analyzed by western blotting for the siRNA on-target and off-target molecules **a** or immunoprecipitated with anti-ABCA1 antibody and the immunocomplexes were analyzed by western blotting with anti-ABCA1, anti-pSer/Thr, or anti-CSN3 antibodies **b**. **c**, **d** All the conditions were the same as in **b** except that cells were assayed for cholesterol efflux **c** or foam cell formation **d**. **e** Quiescent MASMCs were treated with and without thrombin (0.5 U/ml) in the presence and absence of MG132 (10 μM) for 4 h, cell extracts prepared, immunoprecipitated with anti-ABCA1 antibody and the immunocomplexes were analyzed by Western blotting with anti-ABCA1, anti-pSer/Thr or anti-CSN3 antibodies. The input protein from these samples was also immunoprobed for ABCA1, CSN3 and β-actin levels. **f** MASMCs that were transfected with pCMV or pCMV-CSN3 vectors were quiesced, treated with and without thrombin (0.5 U/ml) for 2 h and 4 h, cell extracts prepared, immunoprecipitated with anti-ABCA1 antibody and the immunocomplexes were analyzed by western blotting with anti-Cullin3, anti-CSN3, anti-pSer/Thr, or anti-ABCA1 antibodies. The input protein from these samples was immunoprobed for Myc-tag and β-actin. **g** RAW264.7 cells (left panel) and MASMCs (right panel) that were transfected with pCMV or pCMV-CSN3 vectors were quiesced, treated with and without thrombin (0.5 U/ml) for 2 h and 4 h, cell extracts prepared, immunoprecipitated with anti-ubiquitin antibody and the immunocomplexes were analyzed by western blotting using ABCA1 antibody. The input protein from the same cell extracts were also immunoprobed for ABCA1 levels and CSN3 overexpression (Myc-tag). **h** RAW264.7 cells were treated with and without thrombin (0.5 U/ml) in the presence and absence of MG132 (10 μM) for 2 h, cell extracts prepared, immunoprecipitated with anti-ABCA1 antibodies and the immunocomplexes were immunoblotted sequentially with anti-Ubiquitin, anti-pSer/Thr, anti-CSN3, anti-Cullin3 and anti-ABCA1 antibodies. The input protein from the same cell extracts was immunoprobed for β-actin levels. The bar graphs represent Mean ± SD values of three experiments. $^{*}p < 0.01$ versus siControl; $^{\#}p < 0.01$ versus siControl + Thrombin. Ub-ABCA1, Ubiquitinated ABCA1.

degradation by proteasome pathway in response to thrombin [15]. Similar to macrophages, the mechanistic role of CSN3 in ABCA1 protection appears to be the same in VSMCs as thrombin-induced degradation of ABCA1 correlated with its phosphorylation and dissociation from CSN3 in these cells. Besides, although depletion of CSN3 levels enhanced thrombin-induced ABCA1 degradation and inhibited cholesterol efflux, its overexpression protected ABCA1 from thrombin-induced degradation and restored cholesterol efflux. In addition, although downregulation of CSN3 levels enhanced thrombin-induced foam cell formation, its overexpression attenuated this effect. Based on all these findings, it is likely that in resting macrophages, ABCA1 is nonphosphorylated and remained associated with CSN3 while in response to thrombin, it is phosphorylated by Par1-$G\alpha_{12}$-Pyk2-Gab1-PKCθ signaling, which appears to be required for its dissociation from CSN3 before being ubiquitinated by Cullin3 and degraded. In view of our previous findings [15] and present observations, it may be interpreted that phosphorylation of ABCA1 is a triggering event in its dissociation from CSN3 and association with Cullin3, leading to its ubiquitination and degradation in response to atherogenic stimulants such as thrombin or HFD. In fact, the observations that overexpression of CSN3 inhibits thrombin-induced ABCA1 phosphorylation and its association with Cullin3 suggest that both CSN3 and Cullin3 interact with ABCA1 and their interaction was dependent on the phosphorylation state of ABCA1. In other words, although nonphosphorylated ABCA1 favors its interaction with CSN3, phosphorylated ABCA1 exhibits preference to bind with Cullin3. Under forced expression of CSN3, its cellular levels increase substantially, which in turn, could sequester ABCA1 from being phosphorylated by PKCθ and associated with Cullin3. Besides macrophages, thrombin also induced ABCA1 phosphorylation and its dissociation from CSN3, leading to its degradation in VSMCs and these effects were also dependent on activation of Par1-$G\alpha_{12}$-Pyk2-Gab1-PKCθ signaling in these cells. Based on these observations, it is likely that a similar mechanism of ABCA1 phosphorylation, its dissociation from CSN3 and association with Cullin3, facilitating its ubiquitination and degradation might be triggered by atherogenic stimulants in VSMCs as well. Even more interestingly, although both CSN3 and ABCA1 were found to be colocalized in human non-lesion coronary artery sections, they both were found to be decreased and dissociated from each other in lesion containing human coronary artery sections. In view of all these observations, CSN3 appears to protect ABCA1 by forming a complex and apparently atherogenic stimulants disrupt their interactions rendering ABCA1 vulnerable for ubiquitination and degradation. It is noteworthy that both in mouse and human atherosclerotic lesions, CSN3 levels were also decreased. This indicates that besides Par1 other factors might also play a role in the disruption of CSN3–ABCA1 complex, perhaps involving other mechanisms such as depletion of CSN3 levels and thereby facilitating ABCA1 susceptible for ubiquitination and degradation. Previously, it was reported that disruption of CSN5 enhances NFκB activation, leading to increased expression of cell adhesion molecules and exacerbating atherogenesis [18]. Besides its role in the suppression of NFκB activation and cell adhesion molecules expression, CSN5 might also be involved in the stabilization of ABCA1 ensuring cholesterol efflux, which remains to be investigated. In contrast to these observations, one other study has demonstrated that depletion of CSN2 levels do not affect ubiquitination and the steady state levels ABCA1 as well as cholesterol efflux [36]. However, these observations were contradictory to an earlier report that showed that CSN3 deubiquitinates and protects ABCA1 from degradation [16]. As our findings reveal that besides CSN3, CSN1, CSN2, and CSN4 were also found in

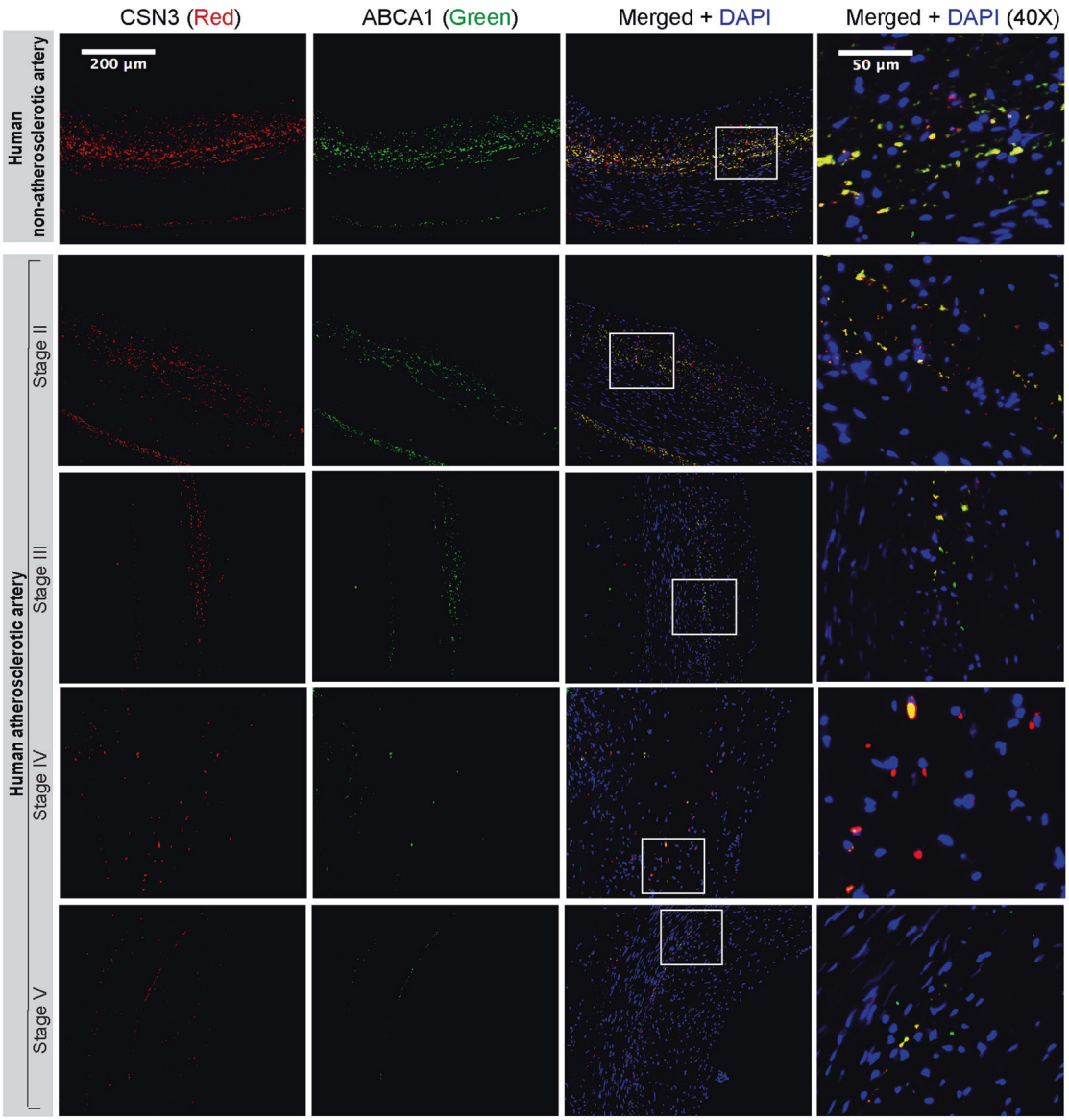

Fig. 8 Depletion of CSN3 and ABCA1 levels in advanced atherosclerotic lesions of human coronary arteries. Human non-lesion and atherosclerotic lesion containing coronary artery sections were stained by double immunofluorescence for CSN3 and ABCA1. The images were captured using a Zeiss AxioCam MRm camera and analyzed by AxioVision 4.7.2 software (Carl Zeiss Imaging Solutions GmbH). The bar graph shows the % CSN3 and ABCA1-positive cells for section. *$p < 0.01$ versus non-atherosclerotic artery.

complex with ABCA1 and thrombin disrupted their association with ABCA1 in a manner that is prevented by MG132, it is likely that CSN3 might be involved in ABCA1 stability and cholesterol efflux as part of CSN holo-complex [37]. Previously, we have reported that Par1-Gα_{12}-Pyk2-Gab1-PKCθ-mediated ATF2 activation via induction of CD36 expression and foam cell formation play a role in diet-induced atherogenesis [38]. In view of our previous findings [15, 38] and present observations, it appears that Par1-Gα_{12}-Pyk2-Gab1-PKCθ signaling via CD36 expression and ABCA1 depletion play a crucial role in atherosclerosis.

In brief, the present study demonstrates for the first time that CSN3 protects ABCA1 from ubiquitination and degradation and thus ensures cholesterol efflux, thereby reducing the risk of developing atherosclerosis. On the other hand, under proatherogenic conditions, ABCA1 gets phosphorylated, which in turn, triggers its dissociation from CSN3 and association with Cullin3 leading to its ubiquitination and degradation, that affects cholesterol efflux. Decreased cholesterol efflux may increase cellular lipid burden and its oxidation facilitating foam cell formation and lesion formation.

Materials and methods

Reagents

Duolink in situ PLA kit (DUO92101), Thrombin (T8885) and Oil Red O (O0625) were purchased from Sigma-Aldrich (St. Louis, MO). MG132 (474790) was bought from Calbiochem (San Diego, CA). Anti-ABCA1 (ab18180), anti-ABCG1 (ab52617), anti-Cullin3 (ab75851), anti-CSN1 (ab194359), anti-CSN2 (ab155920), anti-CSN3 (ab79698), anti-CSN4 (ab139688), anti-Pyk2 (ab32571), anti-pSer/Thr (ab17464) and anti-Ubiquitin (ab7780) antibodies, HDL and LDL/VLDL cholesterol assay kit (ab65390) and triglyceride quantification assay kit (ab65336) were obtained from Abcam (Cambridge, MA). Anti-β-Actin (sc47778), anti-CDK4 (sc23896), anti-CSN3 (sc47961), anti-Gα12 (sc409), anti-GAB1 (sc6292), anti-Par1 (sc5605) and anti-α-tubulin (sc23948) antibodies were bought from Santa Cruz Biotechnology (Santa Cruz, CA). horseradish peroxidase (HRP)-conjugated anti-rabbit IgG (31460) and anti-mouse IgG (31437), DH5α-competent cells (18258-012), lipofectamine 3000 transfection reagent (L3000-015) and Invivofectamine 3.0 reagent (IVF3001) were obtained from Invitrogen (Grand Island, NY). Anti-PKCθ antibody (13643), HRP-conjugated light chain-specific anti-mouse (58802 S) and anti-rabbit IgGs (93702 S) were procured from Cell Signaling Technology (Beverly, MA). OxLDL (BT910) was purchased from Alfa Aesar (Tweksbury, MA). MycDDK-tagged pCMV-CSN3 plasmid (MR206727) was bought from Origene (Rockville, MD). Anti-ubiquitin antibody (P4D1) was purchased from Enzo Life Sciences (Farmingdale, NY). Thioglycollate medium brewer-modified (21176) was obtained from BD Biosciences (San Jose, CA). Control non-targeting siRNA (D-001810-10), mouse CSN3 siRNA (E-047361-00), mouse Gα12 siRNA (L-043467-00) and mouse PKCθ siRNA (L-048426-00) were obtained from Dharmacon RNAi Technologies (Chicago, IL). Mouse Gab1 Silencer Select (ID-S66350), mouse Par1 Silencer Select (ID-S65790), mouse Pyk2 Silencer Select (ID-S72406), mouse CSN3 Silencer Select (ID-S77278, Cat No. 4390771), mouse in vivo negative control (4457289) and mouse in vivo CSN3 (ID-S77278 Cat No. 4457308) siRNAs were purchased from Ambion (Waltham, MA). The Vectashield mounting medium (H-1000) was obtained from Vector Laboratories (Burlingame, CA). [^{3}H]-Cholesterol (S.A. 53 Ci/mmol) was purchased from Perkin Elmer (Waltham, MA). ApoA-I (BT927) was obtained from Biomedical Technologies (Stoughton, MA).

Cell culture

RAW264.7 cells were purchased from American Type Culture Collection (Manassas, VA). Mouse primary aortic smooth muscle cells (MASMCs) were bought from CellBiologics, Inc. (Chicago, IL). RAW264.7 cells and mouse peritoneal macrophages were cultured and maintained in Dulbecco's Modified Eagle Medium (DMEM) containing 10% fetal bovine serum (FBS), 100 units/ml penicillin and 100 µg/ml streptomycin at 37 °C in 95% CO_2 atmosphere. The cells were quiesced overnight in DMEM without serum and used unless otherwise indicated. MASMCs were grown in DMEM/F12 medium containing 10% FBS, 100 units/ml penicillin and 100 µg/ml streptomycin in a humidified CO_2 incubator at 37 °C and used between three and seven passages.

Animals

ApoE$^{-/-}$ mice (Stock no. 002052), Par1$^{-/-}$ mice (Stock no. 00282) and PKCθ$^{-/-}$ mice (Stock no. 005711) were obtained from Jackson Laboratory (Bar Harbor, ME). C57BL/6 mice were obtained from Charles River Laboratories (Wilmington, MA). Mice were bred and maintained according to the guidelines of the Institutional Animal Care and Use Facility of the University of Tennessee Health Science Center, Memphis, TN. Both male and female ApoE$^{-/-}$ mice were fed with CD or WD (TD 88137, Envigo, Indianapolis, IN) for 10 weeks starting from 8 weeks of age to collect aortas and peritoneal macrophages. For other set of experiments, ApoE$^{-/-}$ mice that were fed with WD were also given intravenously in vivo siControl or in vivo siCSN3 (40 µg/20 g body weight) every 7 days for the entire duration of the feeding (2 months) and used. The Institutional Animal Care and Use

Committee of the University of Tennessee Health Science Center, Memphis, TN approved all the experiments involving animals.

Isolation of peritoneal macrophages

To collect peritoneal macrophages, mice were injected intraperitoneally with 1 ml of autoclaved 4% thioglycolate. Four days later, the animals were anaesthetized with ketamine and xylazine and the peritoneal lavage was collected in DMEM. Cells were plated at 3×10^5 cells/cm^2 dish in DMEM containing penicillin (100 units/ml) and streptomycin (100 μg/ml). After 3 h, the floating cells (mostly red blood cells) were removed by washing with cold phosphate-buffered saline (PBS) and the adherent cells (macrophages) were used as needed.

Plasma lipid profiles

Blood was collected into BD Vacutainer Plus plasma tubes (Cat # 367960, BD Biosciences) by cardiac puncture and centrifuged at $1300 \times g$ for 10 min at 4 °C to collect the plasma. Total plasma cholesterol, HDL, LDL, and TG levels were measured by using kits and following the manufacturer's protocols.

Cholesterol efflux assay

RAW264.7 cells and peritoneal macrophages were plated in 12-well plates at a density of 2×10^5 cells/well. Cells were incubated with oxLDL (20 μg/ml) and [^{3}H]-cholesterol (1 μCi/ml) for 24 h followed by washings with PBS for three times. Cells were then equilibrated in serum-free DMEM containing 0.2% fatty acid free-BSA for 2 h. After equilibration, medium was replaced with fresh DMEM containing 0.2% fatty acid free-BSA and 10 μg/ml Apolipoprotein A-I (ApoA-I) and incubation was continued in the presence and absence of thrombin (0.5 U/ml) for 4 h. An aliquot of the efflux medium (100 μl) was removed for radioactivity determination. Cells were then rinsed with PBS, dried and isopropanol was added for overnight extraction of cholesterol at room temperature. An aliquot of the extract (100 μl) was collected for radioactivity determination. Cholesterol efflux was measured as % of total cellular radioactivity released into the medium.

Transfections

RAW264.7 cells were transfected with non-targeting control or Silencer Select siRNA or Smartpool siRNA at a final concentration of 100 nM using Lipofectamine 3000 transfection reagent according to the manufacturer's instructions. For plasmids, cells were transfected with plasmid DNAs at a final concentration of 2.5 μg/well in a 12-well culture plate or 5 μg/60 mm culture dish using Lipofectamine 3000 transfection reagent according to the manufacturer's instructions. After transfections, cells were recovered in complete medium, growth-arrested for 12 h in serum-free medium and used as required.

Immunoprecipitation

Cell or tissue extracts were prepared by lysing cells for 30 min on ice or homogenizing tissues for 53 sec with 2753 total round per run (gentleMACS Octo Dissociator with Heaters, Cat # 130-096-427) in lysis buffer (PBS, 1% NP40, 0.5% sodium deoxycholate, 0.1% sodium dodecyl sulfate (SDS), 100 μg/ml PMSF, 100 μg/ml aprotinin, 1 μg/ml leupeptin, and 1 mM sodium orthovanadate) and cleared by centrifugation at 12,000 rpm for 20 min at 4 °C. Protein concentration was determined using Micro BCA Protein Assay Kit (Pierce). The cell or tissue extracts containing an equal amount of protein from control and the indicated treatments were incubated with the indicated antibodies overnight at 4 °C, followed by incubation with protein A/G-Sepharose CL-4B beads for 2 h with gentle rocking at room temperature. The beads were collected by centrifugation at 1000 rpm for 1 min at 4 °C and washed four times with lysis buffer and once with PBS. The immunocomplexes were released by heating the beads in 40 μl of Laemmli sample buffer and analyzed by western blotting for the indicated molecules using their specific antibodies.

Western blot analysis

Cell or tissue extracts consisting of equal amount protein from control and each treatment were resolved by electrophoresis on 0.1% SDS and 8% or 10% polyacrylamide gels. The proteins were transferred electrophoretically onto a nitrocellulose membrane. After blocking in 5% (w/v) non-fat dry milk, the membrane was incubated with the appropriate primary antibody (1:1000 dilution) followed by incubation with horseradish peroxidase-conjugated secondary antibody (1:5000 dilution). The antigen–antibody complexes were detected with the enhanced chemiluminescence detection reagent kit (GE Healthcare).

Foam cell formation assay

RAW264.7 cells, mouse peritoneal macrophages or mouse aortic smooth muscle cells that were treated with and without thrombin (0.5 U/ml) for the indicated time periods were incubated with oxLDL (10 μg/ml) for 6 h at 37 °C. Cells were then fixed with 4% paraformaldehyde for 30 min, stained with Oil red O for 15 min and counter-stained with hematoxylin. Cell staining was observed under

a Nikon Eclipse TS100 microscope with ×20/0.4 magnification and the images were captured with a Nikon Digital Slight DSL3 camera. After capturing the images, the Oil red O stain was eluted by incubating the slides with isopropanol for 15 min at room temperature and the optical density was measured at 500 nm in a SpectraMax 190 spectrophotometer (Molecular Devices).

Preparation of siRNA for injecting into mice

In brief, siRNA was mixed in complexation buffer at 1:1 ratio followed by remixing the diluted siRNA with Invivofectamine 3.0 by 1:1 ratio and then vortexed immediately to ensure Invivofectamine 3.0-siRNA complexation. Invivofectamine 3.0-siRNA mixture was incubated at 50 °C for 30 min. The Invivofectamine 3.0-siRNA complex was further diluted by six times by adding sterile PBS and injected intravenously into mice.

Proximity ligation assay

The interaction between endogenous CSN3 and ABCA1 was analyzed by using in situ proximity ligation assay kit (Duolink PLA kit; Sigma) as described previously [39]. In brief, after appropriate treatments, RAW264.7 cells were fixed with 3.7% paraformaldehyde for 15 min, permeabilized in 0.3% Triton X100 for 15 min and blocked with 3% BSA for 1 hr. The cells were then incubated with mouse anti-ABCA1 (1:100) and rabbit anti-CSN3 (1:100) antibodies for overnight at 4 °C followed by incubation with goat anti-mouse secondary antibody conjugated with oligonucleotide PLA probe Plus and goat anti-rabbit secondary antibody conjugated with oligonucleotide PLA probe Minus, respectively. The cells were then incubated with a ligation solution for 30 min at 37 °C followed by a rolling-circle amplification of ligated oligonucleotide probes. A fluorescently labeled complementary oligonucleotide detection probe was used to amplify the oligonucleotides conjugated to the secondary antibodies. After washing with wash buffer, the slides were mounted with a mounting media containing DAPI. PLA signals were examined using a Zeiss inverted fluorescence microscope (AxioObserver. Z1; ×100/0.045NA) and the fluorescence images were captured using Zeiss AxioCam MRm camera and microscope operating image analysis software ZEN Pro V2.0 software.

Enface staining

Aortas were excised, cleaned from fat tissue, opened longitudinally and fixed in 10% formalin overnight followed by staining with 0.5% Oil red O. The pictures were taken using Nikon D7100 camera and the percent surface area occupied by the lesions was measured using the NIH ImageJ.

Aortic root sections

For immunohistochemistry and immunofluorescence staining, mice were perfused with 4% paraformaldehyde and the hearts were fixed in OCT. Sequential 10-μm aortic root sections were cut from the point of appearance of the aortic valve leaflets with a Leica CM3050S cryostat machine (Leica Biosystems, Wetzlar, Germany).

Oil Red O staining

The aortic root sections were fixed with 10% formaldehyde solution, washed with PBS, rinsed with 60% isopropanol and stained with Oil red O for 15 min followed by counterstaining with Haematoxylin. The sections were observed under a Nikon Eclipse 50i microscope with ×4/0.1 NA and the images were captured with a Nikon Digital Sight DS-L1 camera.

Immunofluorescence staining

The collection of human normal and atherosclerotic lesion containing coronary artery sections and the classification of the lesion grades were described previously [40]. The studies on the use of human tissue sections were approved by IRB of UTHSC, Memphis, TN. The mouse aortic root cross-sections were fixed with acetone/methanol (1:1), permeabilized with Triton X100, blocked with 3% BSA containing 5% goat serum. The human normal and atherosclerotic lesion containing coronary artery sections were deparaffinized with xylene and then treated with antigen-unmasking solution for 15 min at 95 °C. The sections were then permeabilized with 0.5% Triton X100 for 15 min, and blocking in normal goat serum. After blocking, sections were incubated with mouse anti-human ABCA1 in combination with rabbit anti-human CSN3 antibodies at 1:100 dilution, followed by incubation with Alexa Fluor 488-conjugated goat anti-mouse and Alexa Fluor 568-conjugated goat anti-rabbit secondary antibodies at 1:500 dilution. The sections were washed with PBS, counterstained with Hoechst, mounted with a cover slip using ProLong Gold antifade reagent and observed under a Zeiss inverted microscope (AxioObserver.Z1; ×10/0.25 NA). The fluorescence images were captured using Zeiss AxioCam MRm camera and analyzed by AxioVision 4.7.2 software (Carl Zeiss Imaging Solutions GmbH).

Statistics

All the in vitro experiments were repeated three times. The treatment effects were analyzed by student *t* test for two group comparisons and one-way analysis of variance (ANOVA) followed by Bonferroni post hoc test for

multiple group comparisons. In the case of in vivo experiments, a minimum of seven mice were included in each group and the normality of the data (by D'Agostino-Pearson normality test) and the equality of group variance (by F test) tests were analyzed using GraphPad Prism v 8.00 software. The normally distributed data with similar variance were analyzed by one-way ANOVA followed by Fisher's Least Significant Difference post hoc test or two-tailed student t test. The data are presented as Mean ± SD and the p values < 0.05 are considered statistically significant.

Acknowledgements The present work was supported by grants HL103575 and HL069908 from National Institutes of Health to GN Rao.

Compliance with ethical standards

Conflict of interest The authors declare that they have no conflict of interest.

Publisher's note Springer Nature remains neutral with regard to jurisdictional claims in published maps and institutional affiliations.

References

1. Tabas I. Cholesterol in health and disease. J Clin Invest. 2002; 110:583–90.
2. Trapani L, Segatto M, Pallottini V. Regulation and deregulation of cholesterol homeostasis: the liver as a metabolic "power station". World J Hepatol. 2012;4:184–90.
3. Phillips MC. Molecular mechanisms of cellular cholesterol efflux. J Biol Chem. 2014;289:24020–9.
4. Tall AR, Yvan-Charvet L, Terasaka N, Pagler T, Wang N. HDL, ABC transporters, and cholesterol efflux: implications for the treatment of atherosclerosis. Cell Metab. 2008;7:365–75.
5. Chiang JY. Bile acids: regulation of synthesis. J Lipid Res. 2009;50:1955–66.
6. Ceccanti M, Cambieri C, Frasca V, Onesti E, Biasiotta A, Giordano C, et al. A novel mutation in ABCA1 gene causing tangier disease in an italian family with uncommon neurological presentation. Front Neurol. 2016;7:185.
7. Yin K, Liao DF, Tang CK. ATP-binding membrane cassette transporter A1 (ABCA1): a possible link between inflammation and reverse cholesterol transport. Mol Med. 2010;16:438–49.
8. Guo L, Chen CH, Zhang LL, Cao XJ, Ma QL, Deng P, et al. IRAK1 mediates TLR4-induced ABCA1 downregulation and lipid accumulation in VSMCs. Cell Death Dis. 2015;6:e1949.
9. Zhu Y, Liao H, Xie X, Yuan Y, Lee TS, Wang N, et al. Oxidized LDL downregulates ATP-binding cassette transporter-1 in human vascular endothelial cells via inhibiting liver X receptor (LXR). Cardiovasc Res. 2005;68:425–32.
10. Wang X, Collins HL, Ranalletta M. Fuki IV, Billheimer JT, Rothblat GH, et al. Macrophage ABCA1 and ABCG1, but not SR-BI, promote macrophage reverse cholesterol transport in vivo. J Clin Invest. 2007;117:2216–24.
11. Calkin AC, Tontonoz P. Liver x receptor signaling pathways and atherosclerosis. Arterioscler Thromb Vasc Biol. 2010;30:1513–8.
12. Ogura M, Ayaori M, Terao Y, Hisada T, Iizuka M, Takiguchi S, et al. Proteasomal inhibition promotes ATP-binding cassette transporter A1 (ABCA1) and ABCG1 expression and cholesterol efflux from macrophages in vitro and in vivo. Arterioscler Thromb Vasc Biol. 2011;31:1980–7.
13. Westerterp M, Murphy AJ, Wang M, Pagler TA, Vengrenyuk Y, Kappus MS, et al. Deficiency of ATP-binding cassette transporters A1 and G1 in macrophages increases inflammation and accelerates atherosclerosis in mice. Circ Res. 2013;112:1456–65.
14. Huang L, Fan B, Ma A, Shaul PW, Zhu H. Inhibition of ABCA1 protein degradation promotes HDL cholesterol efflux capacity and RCT and reduces atherosclerosis in mice. J Lipid Res. 2015;56: 986–97.
15. Raghavan S, Singh NK, Mani AM, Rao GN. Protease-activated receptor 1 inhibits cholesterol efflux and promotes atherogenesis via cullin 3-mediated degradation of the ABCA1 transporter. J Biol Chem. 2018;293:10574–89.
16. Azuma Y, Takada M, Maeda M, Kioka N, Ueda K. The COP9 signalosome controls ubiquitinylation of ABCA1. Biochem Biophys Res Commun. 2009;382:145–8.
17. Asare Y, Shagdarsuren E, Schmid JA, Tilstam PV, Grommes J, El Bounkari O, et al. Endothelial CSN5 impairs NF-κB activation and monocyte adhesion to endothelial cells and is highly expressed in human atherosclerotic lesions. Thromb Haemost. 2013;110:141–52.
18. Asare Y, Ommer M, Azombo FA, Alampour-Rajabi S, Sternkopf M, Sanati M, et al. Inhibition of atherogenesis by the COP9 signalosome subunit 5 in vivo. Proc Natl Acad Sci USA. 2017;114:E2766E2775.
19. Korczeniewska J, Barnes BJ. Corrected and Republished from: The COP9 Signalosome Interacts with and Regulates Interferon Regulatory Factor 5 Protein Stability. Mol Cell Biol. 2018;38: e00493–17.
20. Zarich N, Anta B, Fernández-Medarde A, Ballester A, de Lucas MP, Cámara AB, et al. The CSN3 subunit of the COP9 signalosome interacts with the HD region of Sos1 regulating stability of this GEF protein. Oncogenesis. 2019;8:2.
21. Bech-Otschir D, Seeger M, Dubiel W. The COP9 signalosome: at the interface between signal transduction and ubiquitin-dependent proteolysis. J Cell Sci. 2002;115:467–73.
22. Schweitzer K, Bozko PM, Dubiel W, Naumann M. CSN controls NFκB by deubiquitination of IκBα. EMBO J. 2007;26:1532–41.
23. Lim SO, Li CW, Xia W, Cha JH, Chan LC, Wu Y, et al. Deubiquitination and Stabilization of PD-L1 by CSN5. Cancer Cell. 2016;30:925–39.
24. Simoneau M, Boulanger J, Coulombe G, Renaud MA, Duchesne C, Rivard N. Activation of Cdk2 stimulates proteasome-dependent truncation of tyrosine phosphatase SHP-1 in human proliferating intestinal epithelial cells. J Biol Chem. 2008;283:25544–56.
25. Yan J, Walz K, Nakamura H, Carattini-Rivera S, Zhao Q, Vogel H, et al. COP9 signalosome subunit 3 is essential for maintenance of cell proliferation in the mouse embryonic epiblast. Mol Cell Biol. 2003;23:6798–808.
26. Wang R, Wu W, Li W, Huang S, Li Z, Liu R, et al. Activation of NLRP3 inflammasome promotes foam cell formation in vascular smooth muscle cells and atherogenesis Via HMGB1. J Am Heart Assoc. 2018;7:e008596.
27. Allahverdian S, Chaabane C, Boukais K, Francis GA, Bochaton-Piallat ML. Smooth muscle cell fate and plasticity in atherosclerosis. Cardiovasc Res. 2018;114:540–50.
28. Rosenson RS, Brewer HB Jr, Davidson WS, Fayad ZA, Fuster V, Goldstein J, et al. Cholesterol efflux and atheroprotection: advancing the concept of reverse cholesterol transport. Circulation. 2012;125:1905–19.
29. Fielding CJ, Fielding PE. Intracellular cholesterol transport. J Lipid Res. 1997;38:1503–21.
30. Ishiguro H, Yoshida H, Major AS, Zhu T, Babaev VR, Linton MF, et al. Retrovirus-mediated expression of apolipoprotein A-I in

the macrophage protects against atherosclerosis in vivo. J Biol Chem. 2001;276:36742–8.
31. Stary HC, Chandler AB, Glagov S, Guyton JR, Insull W Jr, Rosenfeld ME, et al. A definition of initial, fatty streak, and intermediate lesions of atherosclerosis. A report from the Committee on Vascular Lesions of the Council on Arteriosclerosis, American Heart Association. Arterioscler Thromb. 1994;14:840–56.
32. Tabas I. Cholesterol and phospholipid metabolism in macrophages. Biochim Biophys Acta. 2000;1529:164–74.
33. Schweitzer K, Naumann M. CSN-associated USP48 confers stability to nuclear NF-κB/RelA by trimming K48-linked Ub-chains. Biochim Biophys Acta. 2015;1853:453–69.
34. Aiello RJ, Brees D, Bourassa PA, Royer L, Lindsey S, Coskran T, et al. Increased atherosclerosis in hyperlipidemic mice with inactivation of ABCA1 in macrophages. Arterioscler Thromb Vasc Biol. 2002;22:630–7.
35. Li D, Xiong Q, Peng J, Hu B, Li W, Zhu Y, et al. Hydrogen sulfide up-regulates the expression of ATP-binding cassette transporter A1 via promoting nuclear translocation of PPARα. Int J Mol Sci. 2016;17:E635.
36. Zhang M, Li L, Xie W, Wu JF, Yao F, Tan YL, et al. Apolipoprotein A-1 binding protein promotes macrophage cholesterol efflux by facilitating apolipoprotein A-1 binding to ABCA1 and preventing ABCA1 degradation. Atherosclerosis. 2016;248:149–59.
37. Milic J, Tian Y, Bernhagen J. Role of the COP9 signalosome (CSN) in cardiovascular diseases. Biomolecules. 2019;9:E217.
38. Raghavan S, Singh NK, Gali S, Mani AM, Rao GN. Protein kinase Cθ via activating transcription factor 2-mediated CD36 expression and foam cell formation of Ly6C(hi) cells contributes to atherosclerosis. Circulation. 2018;138:2395–412.
39. Janjanam J, Zhang B, Mani AM, Singh NK, Traylor JG Jr, Orr AW, et al. LIM and cysteine-rich domains 1 is required for thrombin-induced smooth muscle cell proliferation and promotes atherogenesis. J Biol Chem. 2018;293:3088–103.
40. Funk SD, Yurdagul A Jr, Albert P, Traylor JG Jr, Jin L, Chen J, et al. EphA2 activation promotes the endothelial cell inflammatory response: a potential role in atherosclerosis. Arterioscler Thromb Vasc Biol. 2012;32:686–95.